

# Molecular Mechanisms of Action and *In Vivo* Validation of an M<sub>4</sub> Muscarinic Acetylcholine Receptor Allosteric Modulator with Potential Antipsychotic Properties

Katie Leach<sup>1</sup>, Richard E Loiacono<sup>1</sup>, Christian C Felder<sup>2</sup>, David L McKinzie<sup>2</sup>, Adrian Mogg<sup>2</sup>, David B Shaw<sup>2</sup>, Patrick M Sexton<sup>1</sup> and Arthur Christopoulos<sup>\*1</sup>

<sup>1</sup>Drug Discovery Biology and Department of Pharmacology, Monash Institute of Pharmaceutical Sciences, Monash University, Melbourne, Vic., Australia; <sup>2</sup>Neuroscience Division, Eli Lilly & Co., Indianapolis, IN, USA

We recently identified LY2033298 as a novel allosteric potentiator of acetylcholine (ACh) at the M<sub>4</sub> muscarinic acetylcholine receptor (mAChR). This study characterized the molecular mode of action of this modulator in both recombinant and native systems. Radioligand-binding studies revealed that LY2033298 displayed a preference for the active state of the M<sub>4</sub> mAChR, manifested as a potentiation in the binding affinity of ACh (but not antagonists) and an increase in the proportion of high-affinity agonist–receptor complexes. This property accounted for the robust allosteric agonism displayed by the modulator in recombinant cells in assays of [<sup>35</sup>S]GTPγS binding, extracellular regulated kinase 1/2 phosphorylation, glycogen synthase kinase 3β phosphorylation, and receptor internalization. We also found that the extent of modulation by LY2033298 differed depending on the signaling pathway, indicating that LY2033298 engenders functional selectivity in the actions of ACh. This property was retained in NG108-15 cells, which natively express rodent M<sub>4</sub> mAChRs. Functional interaction studies between LY2033298 and various orthosteric and allosteric ligands revealed that its site of action overlaps with the allosteric site used by prototypical mAChR modulators. Importantly, LY2033298 reduced [<sup>3</sup>H]ACh release from rat striatal slices, indicating retention of its ability to allosterically potentiate endogenous ACh *in situ*. Moreover, its ability to potentiate oxotremorine-mediated inhibition of condition avoidance responding in rodents was significantly attenuated in M<sub>4</sub> mAChR knockout mice, validating the M<sub>4</sub> mAChR as a key target of action of this novel allosteric ligand.

*Neuropsychopharmacology* (2010) **35**, 855–869; doi:10.1038/npp.2009.194; published online 25 November 2009

**Keywords:** allosteric modulation; drug discovery; functional selectivity; schizophrenia

## INTRODUCTION

The five muscarinic acetylcholine receptors (mAChRs) have been implicated in numerous diseases, including neurodegenerative and psychiatric disorders (Wess *et al*, 2007). In particular, the M<sub>1</sub> and M<sub>4</sub> mAChRs have been associated with neurological illnesses, as they are widely expressed throughout the central nervous system (Bymaster *et al*, 2003; Wess *et al*, 2003) and are involved in cognitive processes such as attention, learning, and memory (Hasselmo, 2006; Hasselmo and Giocomo, 2006); drugs that selectively target these receptors may thus be useful in the treatment of diseases such as Alzheimer's disease and schizophrenia, in which cognitive processes are disturbed.

The M<sub>4</sub> mAChR is of particular interest with regards to its involvement in schizophrenia because it has been implicated in the regulation of dopamine levels in the brain (Gomeza *et al*, 1999; Tzavara *et al*, 2004; Zhang *et al*, 2002b). Indeed, M<sub>4</sub> mAChRs and D<sub>1</sub> dopamine receptors are coexpressed throughout the striatum (Bernard *et al*, 1992; Ince *et al*, 1997), and decreased levels of M<sub>4</sub> (and M<sub>1</sub>) mAChRs have been found in postmortem brain tissues of schizophrenic patients (Crook *et al*, 2000, 2001; Dean *et al*, 1996; Deng and Huang, 2005; Scarr *et al*, 2007), suggesting a tightly controlled balance between cholinergic and dopaminergic neurotransmission that may be disrupted in schizophrenia.

Encouragingly, Alzheimer's patients treated with the mixed M<sub>1</sub>/M<sub>4</sub>-preferring mAChR agonist, xanomeline, responded with a reduction in psychotic episodes and improvements in cognitive deficits (Bodick *et al*, 1997a,b). In addition, a recent small-scale study of xanomeline administration to schizophrenic patients revealed significant attenuation of negative and cognitive symptoms (Shekhar *et al*, 2008). Unfortunately, xanomeline is not sufficiently selective for the M<sub>1</sub>/M<sub>4</sub> mAChRs over other

\*Correspondence: Professor A Christopoulos, Drug Discovery Biology, Monash Institute of Pharmaceutical Sciences, Monash University, 381 Royal Parade, Melbourne, Vic. 3800, Australia, Tel: +613 9905 3817, Fax: +613 9905 5953, E-mail: arthur.christopoulos@med.monash.edu.au

Received 8 September 2009; revised 29 October 2009; accepted 29 October 2009

subtypes to avoid peripheral mAChR side effects (Bodick *et al*, 1997a, b), which are a common obstacle to the clinical development of mAChR-based drugs. Indeed, the development of highly selective mAChR ligands is impeded by the fact that all mAChR subtypes share high sequence homology within the orthosteric (ie the endogenous agonist-binding site of these receptors). Consequently, recent drug discovery efforts have focused on exploiting novel allosteric-binding sites on these, and other, G protein-coupled receptors (GPCRs) in an effort to attain greater selectivity by targeting regions that are more likely to diverge in sequence from other receptor subtypes (Conn *et al*, 2009; Gregory *et al*, 2007; May *et al*, 2007b).

Although allosteric modulators of GPCRs offer great promise as therapeutics, the molecular mechanisms that govern their pharmacodynamic properties and how these translate to therapeutic efficacy remain relatively unexplored. In addition, reports of allosteric GPCR modulators with the potential to also activate the receptor in their own right (allosteric agonists) are increasing (Langmead and Christopoulos, 2006), highlighting another layer of complexity that must be considered when screening, validating, and quantifying the actions of such molecules. In this regard, we recently identified LY2033298 (3-amino-5-chloro-6-methoxy-4-methyl-thieno[2,3-b]pyridine-2-carboxylic acid cyclopropylamide) as a novel, selective, positive allosteric modulator of acetylcholine (ACh) at the M<sub>4</sub> mAChR that can express agonism under certain conditions (Chan *et al*, 2008; Nawaratne *et al*, 2008). This molecule also displayed *in vivo* efficacy in preclinical models predictive of antipsychotic drug effects, leading us to hypothesize that selective potentiation and/or activation of M<sub>4</sub> mAChRs may be a novel approach to treating schizophrenia (Chan *et al*, 2008). Despite the exciting potential of these findings, however, a number of key questions remain unresolved, including the actual location of the allosteric site with which LY2033298 interacts on the M<sub>4</sub> mAChR; whether agonism of LY2033298 arises solely from interaction with an allosteric site, or whether the molecule uses the latter site to modulate orthosteric ligands while acting as an agonist through the receptor's orthosteric site; whether allosteric modulation differs with the signaling pathway being activated; and to what extent manifestations of allosteric modulation and/or allosteric agonism identified in recombinant systems are retained in native systems. The aim of this study, therefore, was to address these issues and provide a detailed characterization of the molecular mechanisms that govern the novel allosteric properties of LY2033298.

## MATERIALS AND METHODS

### Materials

NG108-15 cells—American type culture collection (Manassas); FLPIn CHO cells, Gateway cloning vectors/enzymes—Invitrogen (Carlsbad); Dulbecco's Modified Eagle media (DMEM) and fetal bovine serum (FBS)—Gibco (Gaithersburg) and JRH Biosciences (Lenexa), respectively; Bio-Rad protein assay dye—Bio-Rad (Hercules); guanosine 5'-[ $\gamma$ -<sup>35</sup>S]triphosphate ([<sup>35</sup>S]GTP $\gamma$ S) (<1000 Ci/mmol) and [<sup>3</sup>H]choline chloride (80 Ci/mmol)—GE Healthcare (Amersham, UK); [<sup>3</sup>H]N-methylscopolamine ([<sup>3</sup>H]NMS) (<70 Ci/mmol), [<sup>3</sup>H]quinuclidinyl benzilate ([<sup>3</sup>H]QNB) (52 Ci/mmol), UltimaGold, Starscint, Irga-Safe Plus, Optiphas supermix, Microscint-O, and AlphaSc-

reen beads—PerkinElmer (Massachusetts); 96-well GF/C filter plates—Millipore (Watford, UK). SureFire extracellular regulated kinase 1/2 (ERK1/2) and glycogen synthase kinase 3 $\beta$  (GSK-3 $\beta$ ) phosphorylation assay kits were a generous gift from Dr Michael Crouch, TGR Biosciences (Adelaide, Australia). LY2033298 was synthesized at Eli Lilly (Indianapolis) and C<sub>7</sub>/3-phth ((heptane-1,7-bis dimethyl-3'-phthalimidopropyl)-ammonium bromide) was synthesized at Monash University using methods described earlier (Nassif-Makki *et al*, 1999). All other chemicals were from Sigma Chemical Company (St Louis).

### Cell Lines

CHO FLPIn M<sub>4</sub> cell lines were maintained as described earlier (Nawaratne *et al*, 2008). HEK293 FLPIn TRex cells stably expressing the M<sub>4</sub> mAChR were generated according to manufacturer's instructions (Invitrogen) and maintained in high glucose DMEM containing 200  $\mu$ g/ml hygromycin, 10  $\mu$ g/ml blasticidin, 10% tetracycline-free FBS, and 16 mM HEPES. NG108-15 cells were maintained in high glucose DMEM without sodium pyruvate containing 10% FBS, 16 mM HEPES, 5 mM sodium hypoxanthine, 20  $\mu$ M aminopterin, and 0.8 mM thymidine.

### Radioligand-Binding Assays

CHO FLPIn cell membranes were prepared as described earlier (Nawaratne *et al*, 2008). Radioligand dissociation was determined by equilibrating cell membranes (15  $\mu$ g/100  $\mu$ l; 1 h; 37°C) with 2 nM [<sup>3</sup>H]NMS in binding buffer (20 mM HEPES, 100 mM NaCl, 10 mM MgCl<sub>2</sub>, pH 7.4) before distribution of 100  $\mu$ l of the mix into 1 ml (final) buffer containing atropine (10  $\mu$ M) in the absence or presence of modulator using a reverse-time protocol. The time course of 0.2 nM [<sup>3</sup>H]NMS association in the absence and presence of LY2033298 was performed in 0.5 ml buffer at 37°C. For equilibrium binding, cell membranes (15  $\mu$ g) were incubated for 3 h at 37°C with either 0.2 nM [<sup>3</sup>H]NMS or 0.1 nM [<sup>3</sup>H]QNB as described earlier (Nawaratne *et al*, 2008).

### [<sup>35</sup>S]GTP $\gamma$ S Assay

Cell membranes (10 or 35  $\mu$ g for the wild type (WT) or Y<sup>113</sup>C/A<sup>203</sup>G mutant M<sub>4</sub> mAChR, respectively) were equilibrated for 1 h at 30°C with varying concentrations of ligands in binding buffer containing 1  $\mu$ M GDP. [<sup>35</sup>S]GTP $\gamma$ S (0.1 nM) was added to a final volume of 0.2 ml (WT) or 0.5 ml (Y<sup>113</sup>C/A<sup>203</sup>G M<sub>4</sub> mAChR) and membranes were incubated for 30 min. Termination of [<sup>35</sup>S]GTP $\gamma$ S binding was by rapid filtration with a Packard plate harvester onto 96-well GF/C filter plates (WT) or with a Brandel harvester onto GF/B filter paper (Y<sup>113</sup>C/A<sup>203</sup>G mutant M<sub>4</sub> mAChR) followed by three washes with ice cold 0.9% NaCl. Plates or filter paper were dried and 40  $\mu$ l Microscint-O was added to each well, or 4 ml UltimaGold added to each filter, before radioactivity was determined by liquid scintillation counting.

### ERK1/2 Phosphorylation Assays

Cells were seeded at 40 000 (FLPIn CHO M<sub>4</sub>), 30 000 (NG108-15), or 100 000 (FLPIn TRex HEK293 M<sub>4</sub>) cells per well into a transparent 96-well plate and grown overnight. For FLPIn

TRex HEK293 M<sub>4</sub> and NG108-15 cells, wells were coated with poly-D-lysine (50 µg/ml) before seeding. For FlpIn TRex HEK293 M<sub>4</sub> cells, cells were treated overnight with tetracycline (10 or 30 ng/ml) to induce expression of the M<sub>4</sub> mAChR. For interaction studies, antagonist or negative modulator were preincubated with cells for 30 min before the addition of agonist for a further 5 min. For interaction studies in which ACh-stimulated ERK1/2 phosphorylation was measured in the presence of LY2033298, to minimize desensitization, LY2033298 was preincubated with cells for only 1 min before the addition of ACh. All other details are as described earlier (Nawaratne *et al*, 2008).

### GSK-3β Phosphorylation Assays

Stimulation of GSK-3β phosphorylation was performed using FlpIn CHO M<sub>4</sub> cells, as described for ERK1/2 phosphorylation assays with the following exceptions: after agonist stimulation and lysis of cells with SureFire lysis buffer, a mixture of reaction buffer, activation buffer, dilution buffer (all as provided by the manufacturer), and AlphaScreen beads was prepared at a ratio of 90:10:40:1 and was added to cell lysates at a ratio of 7:5 in a 384-well opaque Optiplate under low light conditions, for a total volume of 12 µl per well. Plates were incubated in the dark at 37°C for 2 h before the fluorescence signal was measured on a Fusion-α plate reader (PerkinElmer) using standard AlphaScreen settings.

### Receptor Internalization

Cells were seeded into 48-well plates at  $7.5 \times 10^4$  (FlpIn CHO M<sub>4</sub> cells) or  $5 \times 10^4$  cells (NG108-15 cells) per well (coated with poly-D-lysine for NG108-15 cells) and incubated overnight, washed twice with PBS, and incubated in serum-free media. Receptor internalization assays were performed as described earlier (May *et al*, 2005a).

### [<sup>3</sup>H]ACh Release from Rat Striatal Slices

Sprague-Dawley rats (250–350 g) were killed by exposure to CO<sub>2</sub> followed by cervical dislocation. Striata from two rats were dissected and chopped three times at 150 µm using a McIlwain tissue chopper, each time rotating the tissue through 60°C. Slices were dispersed in HEPES buffer (25 mM HEPES, 128 mM NaCl, 2.4 mM KCl, 3.2 mM CaCl<sub>2</sub>·2H<sub>2</sub>O, 1.2 mM KH<sub>2</sub>PO<sub>4</sub>, 1.2 mM MgSO<sub>4</sub>·7H<sub>2</sub>O, 10 mM glucose, 1 µM physostigmine, pH 7.4) and incubated with [<sup>3</sup>H]choline chloride (100 nM) for 30 min at 37°C. After loading, slices were plated into 96-well GF/C filter plates and washed three times over 15 min with buffer (100 µl/well). After the final wash, buffer (with or without LY2033298 and/or NMS) was added and the plates incubated at 37°C for 5 min. Buffer was then removed into a 96-well collection plate. Slices were stimulated for 5 min with 20 mM KCl (with or without LY2033298 and/or NMS), after which the stimulating buffer was removed into a 96-well collection plate. Optiphase supermix (PerkinElmer) scintillation fluid (170 µl) was added to each well of the collection plates before plates being heat sealed and radioactivity quantified using a Wallac 1450 Microbeta 96-well plate counter. Release of [<sup>3</sup>H]ACh was determined as the total counts per minute released over the 5 min of stimulation, which was

converted to a percentage of the release stimulated by 20 mM KCl. Data points are shown as mean ± SEM of four independent experiments (each with eight or more replicates).

### Conditioned-Avoidance Response

Male M<sub>4</sub> mAChR knockout (KO) and WT (C57/BL6 genetic background), weighing 25–45 g, were maintained on a 12:12 light:dark cycle with free food and water access. Conditioned-avoidance response (CAR) training occurred in sound-attenuated mouse shuttle cages using an automated software system (Graphic State Notation; Coulbourn Instruments, Allentown, PA). Adapted to mice, CAR training was performed similarly to that described by Rorick-Kehn *et al* (2007). Each session consisted of a 2 min adaptation period, followed by 50 trials separated by a 30-s inter-trial interval. Illumination of a houselight and opening of shuttle door signaled trial onset. If the mouse shuttled to the other side within 10 s (avoidance response), the trial ended. If an avoidance response was not made, a 0.75-mA floor shock occurred and remained on until a shuttle was made (escape response) or 10 s elapsed (escape failure).

Drug testing occurred once mice stably achieved ≥90% avoidance responding. Drugs were tested 1–2 times per week, providing that mice achieved 90% avoidance criteria after vehicle injection on the day before. For all qualifying and drug days, mice received oral administration of vehicle or 30 mg/kg LY2033298 (suspended in 1% hydroxyethylcellulose/0.25% polysorbate 80/0.05% antifoam) 60 min before testing. Vehicle or 0.1 mg/kg oxotremorine sesquifumarate (dissolved in normal saline) were delivered subcutaneously, 30 min before testing. Drug testing order was as follows: LY2033298 alone, oxotremorine alone, and the combination of LY2033298 and oxotremorine. All drugs were administered in a volume of 10 ml/kg. Only mice that completed all drug doses were included in the final data. A vehicle dose group was calculated by averaging each of the three qualifying days.

### Data Analysis

Radioligand kinetic experiments were fitted to monoexponential association or decay equations (Motulsky and Christopoulos, 2004) and rate constants determined in the presence of LY2033298 were normalized to those determined in its absence. Competition-binding curves between [<sup>3</sup>H]NMS and ACh in the absence or presence of LY2033298 were initially fitted to a two-site-binding model (Motulsky and Christopoulos, 2004) and subsequently to the following allosteric ternary complex model:

$$Y = \frac{[A] \text{Frac}_{\text{Hi}}}{[A] + \left( \frac{K_a K_b}{\alpha' [B] + K_b} \right) \left( 1 + \frac{[I]}{K_{\text{hi}}} + \frac{[B]}{K_b} + \frac{\alpha [I][B]}{K_{\text{hi}} K_b} \right)} + \frac{[A] (1 - \text{Frac}_{\text{Hi}})}{[A] + \left( \frac{K_a K_b}{\alpha' [B] + K_b} \right) \left( 1 + \frac{[I]}{K_{\text{lo}}} + \frac{[B]}{K_b} + \frac{\alpha [I][B]}{K_{\text{lo}} K_b} \right)} \quad (1)$$

where Y is percentage (vehicle control) binding, [A], [B], and [I] are the concentrations of [<sup>3</sup>H]NMS, LY2033298, and ACh, respectively, K<sub>a</sub> and K<sub>b</sub> are the equilibrium dissociation constants of [<sup>3</sup>H]NMS and LY2033298, respectively, K<sub>hi</sub>

and  $K_{lo}$  are the equilibrium dissociation constants of ACh for the high- and low-affinity receptor state, respectively,  $Frac_{Hi}$  is the proportion of receptors in the high-affinity receptor state, and  $\alpha'$  and  $\alpha$  are the cooperativities between LY2033298 and [ $^3H$ ]NMS or ACh, respectively. Values of  $\alpha$  (or  $\alpha'$ )  $> 1$  denote positive cooperativity; values  $< 1$  (but  $> 0$ ) denote negative cooperativity, and values  $= 1$  denote neutral cooperativity.

Concentration-response curves of the interaction between ACh and LY2033298 in various cell-based signaling assays were globally fitted to the following operational model of allosterism and agonism (Leach *et al*, 2007; see Supplemental data for derivation and meaning of parameters):

Response = Basal +

$$\frac{(E_m - \text{Basal})([A](K_b + \alpha\beta[B]) + \tau_b[B][EC_{50}])}{[EC_{50}](K_b + [B]) + ([A](K_b + \alpha\beta[B]) + \tau_b[B][EC_{50}])} \quad (2)$$

This analysis assumes that the orthosteric ligand, ACh, is a full agonist in the signaling pathway under investigation, which was the case for this study.

All affinity, potency, cooperativity, or operational efficacy parameters were estimated as logarithms (Christopoulos, 1998). Statistical analyses were by one-way analysis of variance and Tukey's multiple comparison post-test was applied, with the exception of the CAR experiments, in which a multivariate analysis of variance (MANOVA) was conducted on percent avoidance responses and escape failures; follow-up-dependent-groups *t*-tests were performed

on significant main effects and interactions involving the independent variables genotype and dose.

## RESULTS

### LY2033298 Exhibits 'Probe Dependence' and Redistributes the Proportion of Receptor-G Protein Complexes

In contrast to orthosteric (competitive) interactions, the magnitude of which is solely determined by the respective binding affinities and concentrations of the interacting ligands, allosteric interactions can display markedly different effects depending on the type of ligand occupying the orthosteric site. This characteristic feature of allosteric interactions is called 'probe dependence' (Kenakin, 2007; Leach *et al*, 2007) because the cooperativity between the two binding sites depends on the properties of the orthosteric ligand used as a probe of receptor binding or function. A striking example of this phenomenon is shown in Figure 1, in which it can be seen that LY2033298 minimally perturbed the binding of two structurally distinct orthosteric antagonists, [ $^3H$ ]NMS and [ $^3H$ ]QNB (Figure 1a), whereas it caused a concentration-dependent increase in the potency of the agonist, ACh, to compete for the binding of [ $^3H$ ]NMS (Figure 1b). The binding cooperativity between LY2033298 and the antagonists can thus be characterized as neutral (vs [ $^3H$ ]QNB) or almost-neutral/weakly negative (vs [ $^3H$ ]NMS), whereas the binding cooperativity with ACh is clearly positive. To delineate the mechanistic basis of the almost-neutral cooperativity between LY2033298 and [ $^3H$ ]NMS, we monitored the effects of the allosteric modulator on the

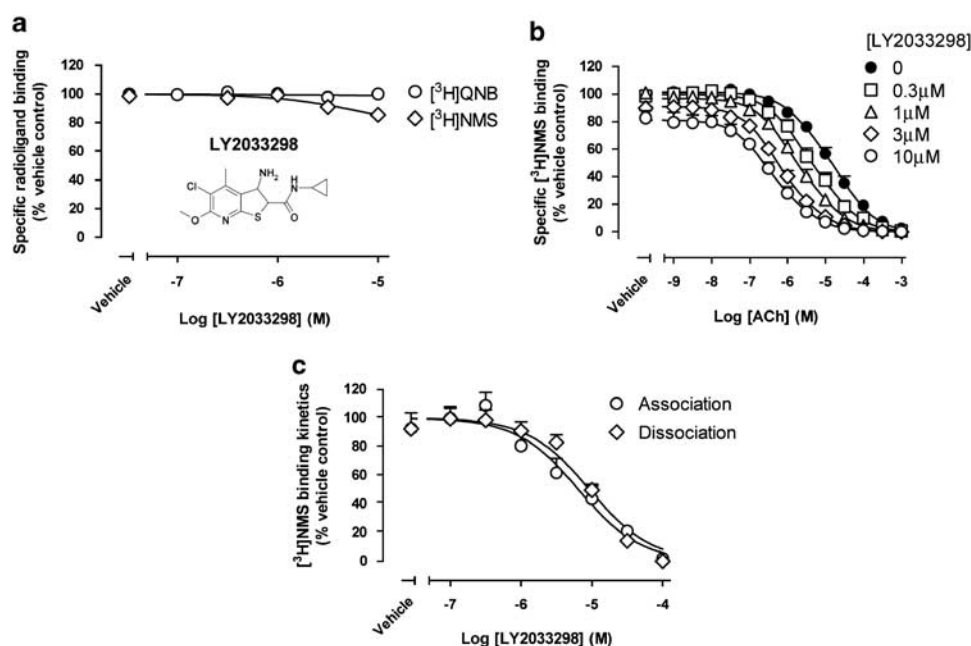


**Figure 1** LY2033298 displays probe dependence when modulating the binding of antagonists and ACh at the M<sub>4</sub> mAChR. (a) Effects of LY2033298 on the equilibrium binding of [ $^3H$ ]NMS or [ $^3H$ ]QNB. Data points represent the mean  $\pm$  SEM of three experiments performed in triplicate. (b) ACh-mediated inhibition of the equilibrium binding of [ $^3H$ ]NMS in the absence or presence of LY2033298. Data points represent the mean  $\pm$  SEM of five experiments performed in triplicate. Curves drawn through the data points represent the best fit of a two-state allosteric ternary complex model (equation (1); Table 1). (c) Concentration-dependent slowing by LY2033298 of the dissociation and apparent association rate of [ $^3H$ ]NMS. Kinetic rate constants were determined in the presence of increasing concentrations of LY2033298 at three time points and normalized as a percentage of the rate constants determined in the absence of modulator (see Materials and methods). Data points represent the mean  $\pm$  SEM of three experiments performed in duplicate.



**Table 1** Binding parameters for the Allosteric Interaction Between LY2033298 and ACh or [<sup>3</sup>H]NMS at the Human M<sub>4</sub> mAChR

Model parameter						
pK <sub>b</sub> <sup>a</sup>			5.34 ± 0.16			
pK <sub>hi</sub> <sup>b</sup>			5.96 ± 0.20			
pK <sub>lo</sub> <sup>c</sup>			4.83 ± 0.17			
	0 <sup>§</sup>	300 nM <sup>§</sup>	1 μM <sup>§</sup>	3 μM <sup>§</sup>	10 μM <sup>§</sup>	
Frac <sub>hi</sub> <sup>d</sup>	0.38 ± 0.14	0.57 ± 0.08	0.63 ± 0.08	0.75 ± 0.09	0.72 ± 0.12	
Logα <sup>e</sup>			1.10 ± 0.30 (α = 12)			
Logα' <sup>f</sup>			−0.34 ± 0.07 (α' = 0.46)			

Parameter values represent the mean ± SEM from five experiments performed in triplicate and analyzed with a two-state allosteric ternary complex model (equation (1)).

<sup>a</sup>Negative logarithm of the equilibrium dissociation constant of LY2033298.

<sup>b</sup>Negative logarithm of the high-affinity equilibrium dissociation constant of ACh.

<sup>c</sup>Negative logarithm of the low-affinity equilibrium dissociation constant of ACh.

<sup>d</sup>Fraction of receptors in the high-affinity receptor state.

<sup>e</sup>Logarithm of the binding cooperativity factor between LY2033298 and ACh.

<sup>f</sup>Logarithm of the binding cooperativity factor between LY2033298 and [<sup>3</sup>H]NMS.

<sup>§</sup>Concentration of LY2033298.

kinetics of association and dissociation of the orthosteric radioligand. As shown in Figure 1c, LY2033298 retarded *both* the dissociation *and* association kinetics of [<sup>3</sup>H]NMS to the same extent and over a similar concentration range. In addition to validating an allosteric mode of action for LY2033298 against [<sup>3</sup>H]NMS, the fact that the modulator changed both the association and dissociation rates of the orthosteric ligand to the same extent explains why no significant effect was noted on the radioligand's affinity at equilibrium—the latter parameter reflects the ratio of the orthosteric ligand's dissociation and association rate constants. Thus, the conformational change engendered in the M<sub>4</sub> mAChR by the binding of LY2033298 is large enough to change the kinetics of orthosteric antagonist binding, but not enough to favor one process (eg dissociation) over another (eg association), leading to neutral cooperativity at equilibrium.

In contrast, the positive cooperativity exerted on the binding of ACh clearly suggests that the conformational change engendered by the modulator is favorable to the binding of the endogenous agonist. Although these assays were performed in the presence of the nonhydrolyzable GTP analog, GppNHp (100 μM), to promote the ground state of the receptor, the competition between ACh and [<sup>3</sup>H]NMS was characterized by biphasic curves with Hill slopes that were significantly less than unity. Application of empirical one- vs two-site binding models, followed by F-test, found that the latter model was more appropriate, indicating that ACh retained the capacity to distinguish between a high- and low-affinity state even in the presence of guanine nucleotide. This finding may be suggestive of a tight coupling between the receptor and its G proteins, similar to what we have earlier found with the adenosine A<sub>1</sub> receptor (May *et al*, 2005b).

Another important observation from the agonist competition experiments was that LY2033298 caused a redistribution of the proportion of the high- and low-affinity-binding sites, with the fraction of high-affinity-binding sites increasing with increasing concentrations of the allosteric modulator (see Supplementary Table 1). The ability of LY2033298 to enhance the proportion of

high-affinity-binding sites was also apparent when [<sup>3</sup>H]QNB was used as the radioligand in ACh competition-binding experiments (data not shown). As a consequence, the competition-binding data were fitted to an allosteric ternary complex model that accommodated the existence of the receptor in two different states (equation 1)) to estimate the affinity of LY2033298 for the allosteric site and its cooperativities with ACh and with [<sup>3</sup>H]NMS. The entire family of curves was globally fitted to the model with all parameters shared across the datasets, with the exception of the fraction of high-affinity states, which was allowed to vary between curves. The results of this analysis are shown in Table 1, in which it can be seen that the effects of LY2033298 are accounted for by a mechanism whereby the modulator binds to the unoccupied receptor with a dissociation constant of ~5 μM (pK<sub>b</sub> = 5.34), potentiates the affinity of ACh for both the high- and low-affinity receptor states by a factor of α = 12, and concomitantly promotes an increase in the high-affinity (presumably G protein-coupled) state of the receptor.

### LY2033298 Potentiates Both the Affinity and the Efficacy of ACh at the M<sub>4</sub> mAChR

Given that the binding data suggested an ability of LY2033298 to potentiate the affinity of ACh as well as promote an increase in receptor-G protein coupling, we performed experiments monitoring the ability of [<sup>35</sup>S]GTPγS to bind to activated Gα proteins as a proximal measure of receptor activation to more directly investigate the consequences of such a mechanism. Figure 2a shows the results of these experiments, in which it can be seen that LY2033298 caused a concentration-dependent increase in receptor signaling even in the absence of ACh, thus acting as an agonist, in addition to allosterically enhancing the potency of the orthosteric agonist. These data were globally fitted to an operational model of allosterism and agonism (equation 2), to yield the parameters shown in Table 2. For this analysis to converge, we fixed the binding affinity of the

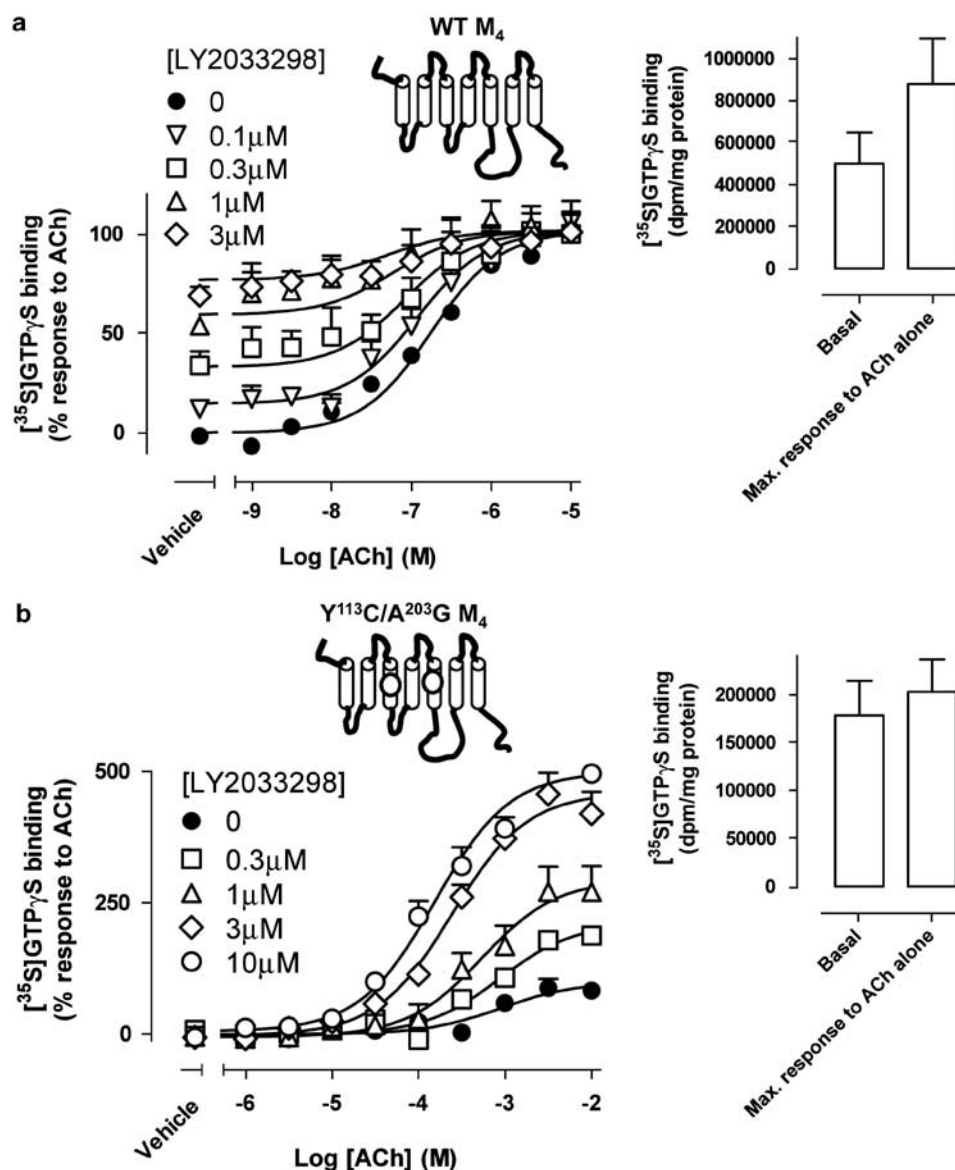


**Figure 2** LY2033298 displays allosteric agonism and potentiates both the affinity and the efficacy of ACh. ACh-mediated [<sup>35</sup>S]GTPγS binding at the WT (a) or a functionally impaired Y<sup>113</sup>C/A<sup>203</sup>G mutant (b) human M<sub>4</sub> mAChR in the absence or presence of LY2033298. Ligands were preincubated with membranes for 1 h at 30°C before the addition of [<sup>35</sup>S]GTPγS for a further 30 min. Data points represent mean + SEM of 3–4 experiments performed in triplicate. Curves drawn through the data points in (a) represent the best fit of an operational allosteric ternary complex model (equation (2); Table 2). Insets indicate the basal and maximal agonist-stimulated levels of [<sup>35</sup>S]GTPγS binding, respectively, for the corresponding receptor construct in dpm/mg protein.

modulator to the pK<sub>b</sub> value determined from the radioligand-binding assays. In the operational model, the agonism of LY2033298 is quantified by the parameter,  $\tau_B$ , which was found to be  $\sim 8$ ;  $\tau$  values  $< 10$  are indicative of partial agonists (Black, 1996). Interestingly, the maximal degree of positive cooperativity between the modulator and ACh from this analysis ( $\alpha\beta$  parameter) was estimated as 36 (Table 2). Given that the allosteric enhancement of ACh-binding affinity,  $\alpha$ , was determined to be 12 from the radioligand-binding assays, our analysis indicates that the additional positive cooperativity observed in the [<sup>35</sup>S]GTPγS assay must result from an allosteric enhancement in the signaling efficacy of ACh (ie  $\beta = 3$ ).

To more directly show that LY2033298 can increase the signaling efficacy of ACh independently of its effects on

orthosteric agonist affinity, these experiments were repeated at an M<sub>4</sub> mAChR with two mutations in key conserved orthosteric site residues (Y<sup>113</sup>C and A<sup>203</sup>G) that result in an almost complete abrogation of the binding and function of ACh (Armbruster *et al*, 2007). As shown in Figure 2b, the significant impairment of ACh signaling at this receptor is rescued by LY2033298, manifesting as an increase in both the potency and, in particular, the maximum response to ACh. This finding is similar to one we made recently with respect to M<sub>4</sub> mAChR-mediated ERK1/2 signaling (Nawaratne *et al*, 2008), indicating that the functional rescue by LY2033298 of impaired orthosteric signaling is likely to apply to multiple signaling pathways. Collectively, these findings are consistent with a mechanism whereby LY2033298 increases the number of high-affinity, G

**Table 2** Operational Model Parameters for the Functional Allosteric Interaction between ACh and LY2033298 at Human M<sub>4</sub> mAChR

Parameter	Ca <sup>2+</sup> mobilization	Internalization	[ <sup>35</sup> S]GTPγS	GSK-3β	ERK1/2
pEC <sub>50</sub> <sup>a</sup>	8.12 ± 0.03	6.01 ± 0.07	6.75 ± 0.08	7.56 ± 0.12	7.80 ± 0.14
pK <sub>b</sub> <sup>b</sup>	5.34	5.34	5.34	5.34	5.34
Logαβ <sup>c</sup>	2.47 ± 0.04 (αβ = 295)	2.90 ± 0.13 (αβ = 794)	1.56 ± 0.18 (αβ = 36)	2.58 ± 0.22 (αβ = 380)	2.57 ± 0.32 (αβ = 372)
Logτ <sub>b</sub> <sup>d</sup>	−1000 <sup>f</sup> (τ <sub>b</sub> = 0)	0.63 ± 0.07 (τ <sub>b</sub> = 4)	0.90 ± 0.04 (τ <sub>b</sub> = 8)	1.38 ± 0.09 (τ <sub>b</sub> = 18)	1.84 ± 0.09 (τ <sub>b</sub> = 51)
E <sub>m</sub> <sup>e</sup>	103 ± 1	24 ± 1	102 ± 2	103 ± 2	65 ± 1

Parameter values represent the mean ± SEM from 3–8 experiments performed in triplicate and analyzed according to equation (2).

<sup>a</sup>Negative logarithm of the concentration of ACh that produces half the maximal agonist response.

<sup>b</sup>Negative logarithm of the equilibrium dissociation constant of LY2033298 (pK<sub>b</sub>); value was fixed to 5.34 as determined from radioligand binding assays at the wild-type M<sub>4</sub> mAChR.

<sup>c</sup>Logarithm of the product of the binding (α) and activation (β) cooperativity factors between ACh and LY2033298. Antilogarithm shown in parentheses.

<sup>d</sup>Logarithm of the operational efficacy parameter of the LY2033298 as an allosteric agonist. Antilogarithm shown in parentheses.

<sup>e</sup>Maximum system response level for the indicated signaling pathway.

<sup>f</sup>Logτ<sub>b</sub> was fixed to −1000 as an arbitrarily low value commensurate with lack of agonism.

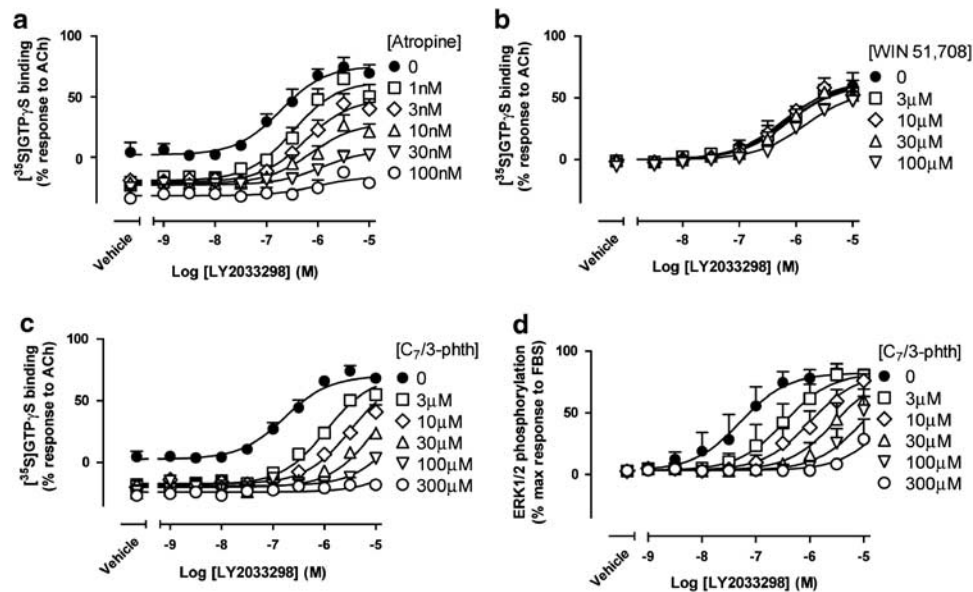


**Figure 3** LY2033298 binds to the M<sub>4</sub> mAChR through a region that overlaps with the prototypical allosteric-binding site. (a–c) LY2033298-stimulated [<sup>35</sup>S]GTPγS binding alone or in the presence of (a) atropine, (b) WIN51708, and (c) C<sub>7</sub>/3-phth. Data points represent mean + SEM of three experiments performed in triplicate. (d) LY2033298-mediated ERK1/2 phosphorylation alone or in the presence of C<sub>7</sub>/3-phth. Data points represent the mean + SEM of three experiments performed in triplicate

protein-coupled, M<sub>4</sub> mAChR states to directly stimulate G protein activation as well as enhancing both the affinity and the efficacy of the endogenous agonist ACh.

### LY2033298 binds to the M<sub>4</sub> mAChR at a Region that Overlaps with the ‘Prototypical’ Allosteric-Binding Site

Extensive mutagenesis studies have determined a function for residues in the second and third extracellular loops and at the top of transmembrane domain VII to be important for the binding of prototypical allosteric modulators such as C<sub>7</sub>/3-phth and gallamine at mAChRs (Ellis *et al*, 1993; Huang *et al*, 2005; Krejci and Tucek, 2001; Leppik *et al*, 1994; May *et al*, 2007a; Prilla *et al*, 2006; Voigtlander *et al*, 2003). Preliminary mutagenesis experiments with LY2033298 also implicated extracellular loop regions in the

actions of the modulator (Chan *et al*, 2008). However, there is another class of ‘atypical’ modulators, such as WIN51708, WIN62577, staurosporine, and KT5720, that bind to a second, currently unresolved, allosteric site on mAChRs (Lanzafame *et al*, 2006; Lazareno *et al*, 2000, 2002). Thus, to gain more definitive insight into which allosteric site is involved in the binding of LY2033298, we exploited the ability of the modulator to also act as an agonist and performed functional interaction studies between this compound and either the classic orthosteric antagonist, atropine, the ‘prototypical-site’ allosteric modulator, C<sub>7</sub>/3-phth, or the ‘second-site’ allosteric modulator, WIN51708.

Figure 3a shows the interaction between LY2033298 and atropine in [<sup>35</sup>S]GTPγS-binding assays. In addition to behaving as an inverse agonist, atropine caused a profound reduction in the maximal agonist effect of LY2033298 with minimal change in its potency. This finding is clearly

inconsistent with a competitive interaction and provides further evidence that LY2033298 mediates its agonist effects from an allosteric site. When these experiments were repeated using WIN51708 as the interacting ligand, a markedly different profile of behavior was noted (Figure 3b). Specifically, WIN51708 had virtually no effect on the shape or location of the LY2033298 concentration-response curve, indicative of neutral cooperativity between two topographically distinct-binding sites. Finally, the interaction between LY2033298 and C<sub>7</sub>/3-phth was investigated (Figure 3c). As with atropine, the allosteric modulator, C<sub>7</sub>/3-phth, was able to reduce constitutive M<sub>4</sub> mAChR-mediated [<sup>35</sup>S]GTPγS binding. However, this effect was accompanied by a significant dextral translocation of the LY2033298 concentration-response curve, suggestive of a competitive interaction. Unfortunately, because of the relatively low potency of the allosteric agonist in this assay, together with solubility limitations, complete concentration-response curves could not be established in the presence of the higher concentrations of C<sub>7</sub>/3-phth, making our conclusion of a competitive interaction speculative. To address this, we repeated the experiments using a second functional assay of receptor activation, that of ERK1/2 phosphorylation (Figure 3d), which is characterized by a higher level of stimulus-response amplification and, accordingly, an increase in the potency of LY2033298 as an agonist. This afforded a greater window for observing translocations in the agonist concentration-response curve and, as shown in Figure 3d, the data were clearly indicative of a competitive interaction. Analysis of these ERK1/2 data according to a simple competitive model of interaction (Motulsky and Christopoulos, 2004) yielded a pK<sub>b</sub> estimate for C<sub>7</sub>/3-phth of 6.26 ± 0.11, which was in good agreement with earlier estimates for the modulator for interaction with the prototypical allosteric site on the M<sub>4</sub> mAChR (Christopoulos *et al*, 1999). It is also in excellent agreement with affinity values determined from application of a simple allosteric ternary complex model (Motulsky and Christopoulos, 2004) to the interaction between C<sub>7</sub>/3-phth and ACh in the current ERK1/2 experiments (6.26 ± 0.05; data not shown). Thus, for the first time, we have identified that LY2033298 binds to and activates the M<sub>4</sub> mAChR through a region on the receptor that must overlap with residues that contribute to the prototypical mAChR allosteric-binding site.

### LY2033298 Allosterically Engenders Functional Selectivity in the Signaling of ACh

Given that allosteric modulators can co-bind with an orthosteric agonist and promote unique changes in receptor conformation, we have recently proposed that there is no *a priori* reason why the resulting conformations should display equivalent degrees of allosteric modulation across different signaling pathways linked to the same receptor in the same cellular background (Leach *et al*, 2007). This phenomenon is referred to as modulator-engendered 'functional selectivity' or 'stimulus-bias' (Urban *et al*, 2007), and has significant implications for the detection and development of allosteric molecules as putative drug candidates. To investigate whether LY2033298 can impose functional selectivity on the actions of ACh, we extended our studies of ACh/LY2033298 functional interactions to incorpo-

rate assays of the phosphorylation of ERK1/2 and GSK-3β, as well as the ability of ACh to promote M<sub>4</sub> mAChR internalization. ERK1/2 and GSK-3β were chosen because they have been implicated as important signaling pathways downstream of receptor activation in a variety of CNS-relevant disorders, including schizophrenia (Beaulieu *et al*, 2009, 2004; Dwivedi *et al*, 2001; Emamian *et al*, 2004; Feng *et al*, 2003; Ikeda *et al*, 2004; Lovestone *et al*, 2007). Receptor internalization was chosen because it is a common mechanism whereby the effects of many GPCR agonists are regulated; the net effect of any receptor-based therapy reflects interplay between acute signaling and longer-term regulatory pathways. For further comparison across pathways, we have also included an analysis of our prior study of the effect of LY2033298 on ACh-mediated intracellular Ca<sup>2+</sup> mobilization (Chan *et al*, 2008).

In agreement with the [<sup>35</sup>S]GTPγS-binding experiments, LY2033298 displayed a robust degree of allosteric agonism for ERK1/2 phosphorylation, GSK-3β phosphorylation, and internalization assays (Figure 4). It should be noted that this was not because of the potentiation by LY2033298 of any trace amounts of endogenous or contaminating ACh, as identical results were obtained in the presence of acetylcholinesterase (Supplementary data Figure 1). In addition to allosteric agonism, LY2033298 potentiated the actions of ACh at all pathways examined. However, application of our operational model of allosterism and agonism to the datasets revealed that the degree of potentiation varied between pathways (Table 2). For instance, in the ERK1/2 and GSK-3β phosphorylation assays, the functional cooperativity ( $\alpha\beta$ ) between LY2033298 and ACh was estimated as 372 and 380, respectively. These values were significantly ( $P < 0.05$ ) higher than that estimated from the [<sup>35</sup>S]GTPγS-binding assays (36), and are thus suggestive of pathway-selective allosteric modulation. However, there is a theoretical rationale for the degree of positive modulation of a given pathway to be correlated with the degree of agonism displayed for that pathway by the allosteric ligand (Hall, 2000). Given that the agonism parameter,  $\tau_b$ , estimated for the ERK1/2 and GSK-3β phosphorylation assays (52 and 18, respectively) was higher than that determined from the [<sup>35</sup>S]GTPγS-binding assays (8), it is possible that the greater degree of positive cooperativity reflects the greater degree of allosteric agonism and that, in the absence of the latter, the positive modulation may actually be less.

In this regard, the analysis of our internalization data and Ca<sup>2+</sup> mobilization data was particularly striking. The former assay was associated with a level of allosteric agonism ( $\tau_b = 4$ ) that was less than that determined in the [<sup>35</sup>S]GTPγS-binding assays, but resulted in the greatest degree of positive modulation observed in any of the assays ( $\alpha\beta = 794$ ); as with the ERK1/2 and GSK-3β assays, this was significantly different ( $P < 0.05$ ) from that determined for the [<sup>35</sup>S]GTPγS-binding assay. With respect to the ability of LY2033298 to potentiate ACh-mediated intracellular Ca<sup>2+</sup> mobilization, we did not see any detectable agonism of the modulator (ie  $\tau_b = 0$ ) in our prior study (Chan *et al*, 2008), but have determined a cooperativity estimate ( $\alpha\beta = 295$ ) that is significantly higher ( $P < 0.05$ ) than that observed for [<sup>35</sup>S]GTPγS binding. Taken together, these results provide the first evidence for pathway-specific allosteric modulation by LY2033298 on the actions of ACh.



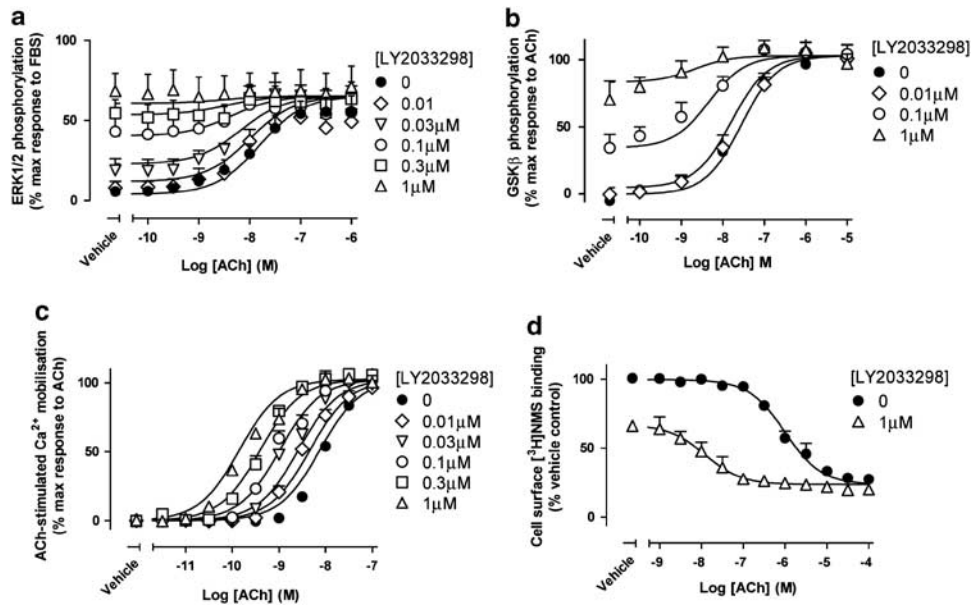


**Figure 4** LY2033298 engenders functional selectivity (stimulus-bias) in the signaling of ACh. ACh-mediated ERK1/2 phosphorylation (a), GSK-3 $\beta$  phosphorylation (b), Ca<sup>2+</sup> mobilisation (c), and receptor internalization (d) in the absence or presence of LY2033298. Cells or membranes expressing the M<sub>4</sub> mAChR were treated with agonist and agonist-stimulated receptor activity was determined as described in Materials and methods. Data shown in (c) are re-plotted from Chan et al (2008). Data points represent the mean  $\pm$  SEM of 3–8 experiments performed in triplicate. Curves drawn through the points are the best fit of an operational ternary complex model (equation (2); Table 2).

### Positive Cooperativity between LY2033298 and Orthosteric Agonists Is Retained *In Situ*, but Greatly Reduced in M<sub>4</sub> mAChR KO Mice

To determine how the allosteric properties of LY2033298 that we identified in the FlpIn CHO cells translate to a native cellular environment, we extended our investigations of the modulator's activity to a neuronal-like cell line, to native brain tissue and finally to behavior in WT and M<sub>4</sub> mAChR KO mice.

We first investigated the effects of LY2033298 on NG108-15 cells, which natively express both rat and mouse mAChRs. To facilitate analysis of the signaling data generated in the NG108-15 cells, we initially determined the affinity of the allosteric modulator for the mouse M<sub>4</sub> receptor alone expressed in CHO K1 cells (data not shown); the resulting pK<sub>b</sub> value,  $5.54 \pm 0.57$  ( $n=3$ ), was not significantly different from that obtained at the human receptor. Subsequently, we chose two signaling assays that were indicative of LY2033298-engendered functional selectivity based on our CHO FlpIn studies (Figure 4), namely ERK1/2 phosphorylation and receptor internalization, and repeated these experiments in the NG108-15 cells. As with the CHO cell studies, LY2033298 caused a robust potentiation of the ability of ACh to promote both ERK1/2 phosphorylation and internalization in the NG108-15 cells (Figure 5a and b). It was noted, however, that the degree of allosteric agonism was markedly reduced in the native cell background, being virtually absent in the internalization assay (Figure 5b). The most likely explanation for the differing strength of LY2033298 agonism between the two cell lines is the lower expression level of M<sub>4</sub> mAChRs in the NG108-15 cells. To confirm the dependence of LY2033298 agonism on receptor expression levels, we generated a

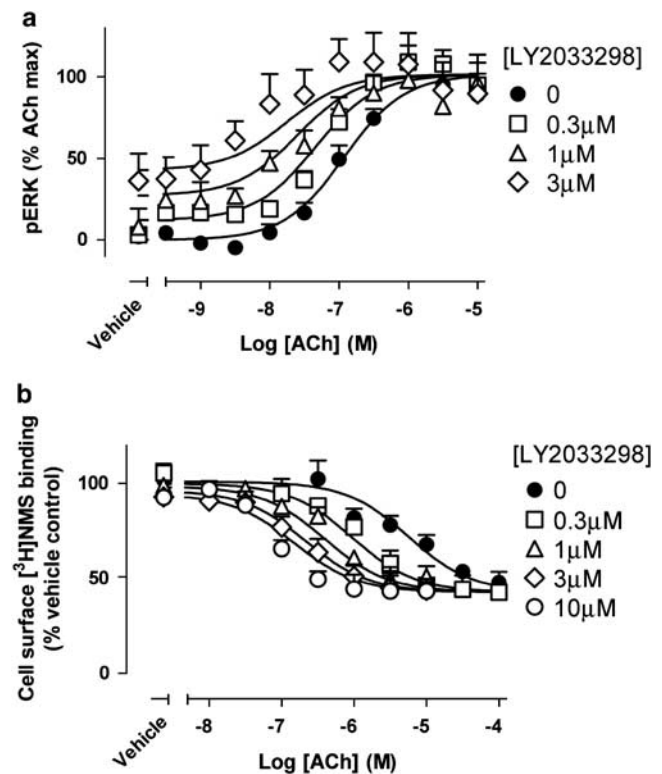


**Figure 5** *In vitro* validation of LY2033298 as an allosteric potentiator in native cells expressing rodent M<sub>4</sub> mAChRs. (a) ERK1/2 phosphorylation and (b) internalization in NG108-15 cells by ACh alone or in the presence of LY2033298. Data points represent the mean  $\pm$  SEM of four experiments performed in triplicate. Curves drawn through the points are the best fit of an operational ternary complex model (equation (2); Table 3).

**Table 3** Operational Model Parameters for the Functional Allosteric Interaction between ACh and LY2033298 in NG108-15 Cells

Parameter	Internalization	ERK1/2
pEC <sub>50</sub> <sup>a</sup>	5.25 ± 0.12	6.93 ± 0.11
pK <sub>b</sub> <sup>b</sup>	5.54	5.54
Log $\alpha\beta$ <sup>c</sup>	1.74 ± 0.12 ( $\alpha\beta = 55$ )	1.34 ± 0.17 ( $\alpha\beta = 22$ )
Log $\tau_b$ <sup>d</sup>	−0.78 ± 0.29 ( $\tau_b = 0.17$ )	0.15 ± 0.06 ( $\tau_b = 1.4$ )
E <sub>m</sub> <sup>e</sup>	43 ± 2	102 ± 3

Parameter values represent the mean ± SEM from four experiments performed in triplicate and analyzed according to equation (2).

<sup>a</sup>Negative logarithm of the concentration of ACh that produces half the maximal agonist response.

<sup>b</sup>Negative logarithm of the equilibrium dissociation constant of LY2033298 (pK<sub>b</sub>); value was fixed to 5.54 as determined at the mouse M<sub>4</sub> mAChR expressed in CHO cells.

<sup>c</sup>Logarithm of the product of the binding ( $\alpha$ ) and activation ( $\beta$ ) cooperativity factors between ACh and LY2033298. Antilogarithm shown in parentheses.

<sup>d</sup>Logarithm of the operational efficacy parameter of the LY2033298 as an allosteric agonist. Antilogarithm shown in parentheses.

<sup>e</sup>Maximum system response level for the indicated signaling pathway.

tetracycline-inducible M<sub>4</sub> mAChR expression system using an HEK293 TRex cell line. As shown in Supplementary data Figure 2, progressive reduction in the expression level of the M<sub>4</sub> mAChR in these cells led to a marked reduction in the efficacy of LY2033298, relative to ACh, as expected.

Subsequent analysis of the NG108-15 cell data according to equation 2 yielded the parameter estimates shown in Table 3. Importantly, the pathway-specific allosteric modulation that was observed in the CHO FlpIn cell line expressing the human M<sub>4</sub> receptor seemed to be retained in the NG108-15 cells; despite displaying minimal agonism for the internalization pathway ( $\tau = 0.2$ ), LY2033298 caused the greater degree of potentiation of this response ( $\alpha\beta = 55$ ) relative to ERK1/2 ( $\alpha\beta = 22$ ). Collectively, these findings suggest that allosteric modulator-mediated functional selectivity can indeed be operative in a native cellular environment.

We next determined the effects of LY2033298 *in situ* by monitoring [<sup>3</sup>H]ACh release in rat striatal slices, a process known to be regulated by presynaptic M<sub>4</sub> autoreceptors (Zhang *et al*, 2002a). A key focus of these experiments was to delineate the extent to which direct allosteric agonism, as opposed to allosteric potentiation of endogenous ACh, was operative in the actions of the modulator in a native tissue environment. To address this, we took advantage of the unique probe-dependent properties of LY2033298 with respect to its interaction with the antagonist, NMS (Figure 1a). Specifically, because our radioligand-binding assays had indicated that NMS and LY2033298 display minimal interaction with one another, we reasoned that any reversal of the effects of the modulator by NMS must be due to inhibition of the actions of endogenous ACh; in contrast, direct allosteric agonism by LY2033298 would be resistant to inhibition by NMS. As shown in Figure 6a, LY2033298 caused a concentration-dependent inhibition of 20 mM KCl-evoked [<sup>3</sup>H]ACh release in rat striatum that was almost completely reversed by NMS, indicating that the major effect of the modulator in this tissue is to potentiate the

effects of endogenous ACh on presynaptic M<sub>4</sub> mAChRs; the antagonist alone also caused a modest increase in [<sup>3</sup>H]ACh release, consistent with an inhibition of endogenous ACh tone. Interestingly, we also noted that a small degree (~20%) of the inhibition of ACh release by LY2033298 could not be abolished in the presence of NMS, suggesting that some direct allosteric agonism by LY2033298 may be retained *in situ*.

Finally, the *in vivo* activity of LY2033298 was measured in a CAR paradigm. Administration of LY2033298 (30 mg/kg) alone did not suppress avoidance responses or increase latency of response in either WT or M<sub>4</sub> mAChR KO mice (Figure 6b and c). A submaximal dose of oxotremorine (0.1 mg/kg) reduced avoidance responses in WT and M<sub>4</sub> mAChR KO mice by ~55 and 35%, respectively. Co-administration of both LY2033298 and oxotremorine significantly reduced avoidance responses in the WT mice, such that they were almost completely lost, and significant escape failures (40%) were observed. In contrast, there was only a slight, but significant, reduction in avoidances, and no escape failures, over and above that produced by oxotremorine alone in the M<sub>4</sub> mAChR KOs. MANOVA results confirmed these observations: principal effects of genotype [F(1,23) = 19.63,  $P < 0.0002$ ] and dose [F(3,69) = 0.0001], as well as a significant interaction of these variables, were found on analysis of avoidance responses [F(3,69) = 13.86,  $P < 0.0001$ ]. A significant Genotype × Dose interaction was revealed on escape failures, with only WT mice expressing escape failures when given the combination of LY2033298 and oxotremorine [F(3,69) = 10.64,  $P < 0.0001$ ].

## DISCUSSION

This study provides novel insights into the molecular mechanisms of action of LY2033298, which, together with a related series of molecules, has recently been proposed as a novel, M<sub>4</sub>-mAChR-selective, tool that may provide a new avenue for the treatment of disorders such as schizophrenia (Chan *et al*, 2008; Shirey *et al*, 2008). We have defined a mechanistic basis for the differential effects of this compound on the binding of orthosteric antagonists compared with agonists such as ACh, have validated pharmacologically that both agonism and modulation by LY2033298 arise from an allosteric site that likely overlaps with the site used by prototypical mAChR modulators, have identified, for the first time, signal pathway-selective allosteric modulation at the M<sub>4</sub> mAChR, and validated this receptor subtype as a key target for LY2033298 in native cellular systems as well as *in vivo*.

One of the great challenges in the detection and validation of novel allosteric modulators as potential drug candidates is the issue of probe dependence (Leach *et al*, 2007). Depending on the nature of the orthosteric ligand, therefore, the resultant pharmacology can vary dramatically. In the case of LY2033298, this was evident when testing the modulator against the antagonists, [<sup>3</sup>H]NMS, or [<sup>3</sup>H]QNB, in which virtually no effect on equilibrium binding was noted, compared with the agonist, ACh, in which marked positive cooperativity was observed. These findings have a number of important implications. First, the lack of affinity modulation of the radioligands clearly indicates that the binding site of LY2033298 does not overlap with the classic

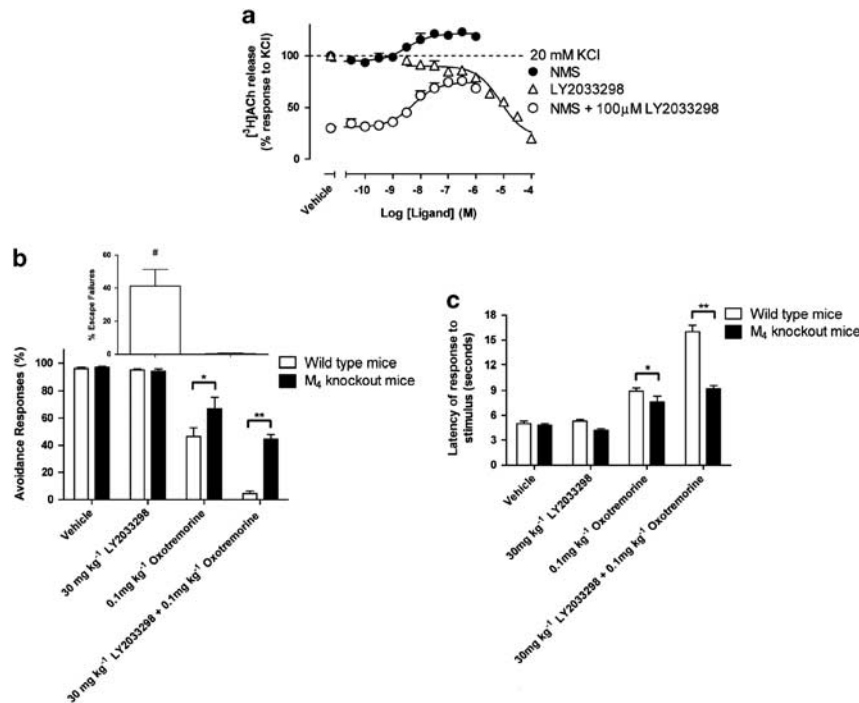


**Figure 6** *In situ* and *in vivo* validation of LY2033298 as an allosteric potentiator at rodent M<sub>4</sub> mAChRs. (a) 20 mM KCl-stimulated [<sup>3</sup>H]ACh release from rat striatal slices in the presence of LY2033298, NMS, or NMS plus 100 μM LY2033298. Data points represent the mean + SEM of four experiments performed with eight replicates. (b) CARs and escape failures and (c) latency in response in WT and M<sub>4</sub> mAChR KO mice after individual dosing of LY2033298 (30 mg/kg) and oxotremorine (0.1 mg/kg), or a combination of LY2033298 and oxotremorine. \**P* < 0.05 oxotremorine alone vs vehicle treatment; \*\**P* < 0.05 combination vs oxotremorine alone; #*P* < 0.05 WT vs M<sub>4</sub> mAChR KO mice. Data are means + SEM.

orthosteric pocket; indeed, the positive cooperativity with ACh means that the modulator prefers to bind to a receptor in which this pocket is occupied by an agonist. Second, if the cooperativity between modulator and orthosteric probe is essentially neutral, as was the case with the antagonists in our study, then the assay will fail to detect the allosteric ligand as having any activity unless a different probe is used; this has important implications for modulator screening. Importantly, our [<sup>3</sup>H]NMS kinetic-binding studies clearly revealed that the modulator was binding allosterically and changing the conformation of the receptor; the mechanistic basis for the neutral cooperativity at equilibrium was that both radioligand association and dissociation were modulated to the same extent over the same concentration range of the modulator. Third, given that [<sup>3</sup>H]NMS and [<sup>3</sup>H]QNB are structurally different (tropate vs benzilate, respectively), yet both exhibited neutral cooperativity with LY2033298 in contrast to ACh, this suggests that the molecular basis for the probe dependence we observed is a sensitivity of the modulator to the conformational state of the receptor (ie active vs inactive).

Further evidence in support of a preferential interaction with an active state of the M<sub>4</sub> mAChR by LY2033298 was evident in the ACh/[<sup>3</sup>H]NMS competition-binding studies, in which the modulator caused an increase in the proportion of the high-affinity state as well as enhancing the binding affinity of ACh. Although the mechanisms that govern the dispersion of agonist affinities across multiple GPCR states in membrane-based radioligand-binding

assays remain unclear, a common interpretation is that this somehow reflects the coupling of the GPCR to its cognate G protein(s) to engender a high-affinity state (Christopoulos and El-Fakahany, 1999). Interestingly, the attendant increase in the proportion of the high-affinity ACh state with increasing concentrations of LY2033298 was also observed in our prior study (Nawaratne *et al*, 2008), but was not factored into our analysis of the interaction at that time because of a limited number of datasets. This likely explains the difference in  $\alpha$  values between that study ( $\alpha = 60$ ) and this study ( $\alpha = 12$ ).

The ability of LY2033298 to act as an agonist in the absence of ACh in various signaling assays was another unambiguous demonstration that the modulator prefers an active receptor state. Importantly, this agonistic property of LY2033298 afforded a unique opportunity to perform functional interaction studies with various ligands to pharmacologically probe the location of the allosteric site with which LY2033298 interacts. The interaction between LY2033298 and C<sub>7</sub>/3-phth was competitive, revealing for the first time that the binding site for LY2033298 must overlap with regions in the extracellular, 'prototypical', allosteric mAChR site used by C<sub>7</sub>/3-phth. This finding is in general agreement with our prior mutagenesis study (Chan *et al*, 2008), which suggested an engagement of the modulator with extracellular loop regions of the M<sub>4</sub> mAChR and an important function of D<sup>432</sup> in the third extracellular loop; this residue has been implicated in the binding of the prototypical modulator, gallamine, to the M<sub>4</sub> mAChR (Gnagey *et al*, 1999). In contrast, the interaction between



LY2033298 and atropine was negatively cooperative, whereas that between LY2033298 and WIN51708 was neutrally cooperative; both findings clearly indicate that LY2033298 does not interact with either the orthosteric site or a second allosteric site on the M<sub>4</sub> mAChR recognized by staurosporine, KT5720, and various WIN compounds (Lanzafame *et al*, 2006; Lazareno *et al*, 2000, 2002).

It should be noted that LY2033298 is not the first agonist of mAChRs reported to interact allosterically with this receptor family. Compounds such as AC-42, 77-LH-28-1, *N*-desmethyloclozapine, TBPB, and McN-A-343 have been earlier classified as 'allosteric agonists' at M<sub>1</sub> and/or M<sub>2</sub> mAChRs (Birdsall *et al*, 1983; Jones *et al*, 2008; Langmead *et al*, 2006; May *et al*, 2007a; Spalding *et al*, 2006; Sur *et al*, 2003). However, the interaction between each of these ligands and orthosteric mAChR ligands is antagonistic, suggesting that they either interact with both the orthosteric and an allosteric site on the mAChR, or otherwise are highly negatively cooperative with orthosteric ligands. Given our recent demonstration that McN-A-343 is actually a 'bitopic' ligand, concomitantly engaging both the orthosteric and allosteric sites on the M<sub>2</sub> mAChR to engender functional selectivity in its actions (Valant *et al*, 2008), it is possible that this bitopic mode may also extend to the aforementioned agonists (Valant *et al*, 2009). In contrast, and based on the pharmacological data presented herein, we propose that LY2033298 exerts both its allosteric agonism and its allosteric modulation solely through interaction with the same allosteric site. In this regard, the molecule is unique and the first example of a 'pure' allosteric agonist of mAChRs.

Another important premise of this study is that the use of quantitative models of allosterism can yield parameters that describe the nature of the interaction and furnish numbers that can guide subsequent structure-activity studies. Application of our operational model of allosterism and agonism to data derived for LY2033298 in various signaling assays revealed the novel finding that the magnitude of the modulation varied depending on the pathway under investigation, that is the allosteric modulator was 'biasing' the stimulus imparted to the receptor by ACh. This property is quantified by the  $\beta$  parameter (efficacy modulation) of our model (Leach *et al*, 2007). On the basis of the data summarized in Table 2, and assuming that  $\alpha = 12$  (affinity modulation) for the interaction between LY2033298 and ACh at the human M<sub>4</sub> mAChR, then  $\beta$  values can be calculated as 3, 25, 31, 32, and 66 for [<sup>35</sup>S]GTP $\gamma$ S binding, Ca<sup>2+</sup> mobilization, ERK1/2 phosphorylation, GSK-3 $\beta$  phosphorylation, and receptor internalization, respectively. To our knowledge, this is the first example of allosteric modulator-engendered functional selectivity in the signaling of ACh at any mAChR. On a practical level, these findings have significant implications because in most instances, it is not possible to link modulator effects on a specific signal pathway to the prediction of therapeutic efficacy, which in turn suggests that novel compound profiling should be as broad as possible.

One means of increasing the translational relevance of findings such as those described above is to assess the activity of novel modulators in native systems. In this regard, two advantages of the NG108-15 cells used in this study were that they endogenously express M<sub>4</sub> mAChRs (albeit rodent receptors), and that the expression level

approximates those found in brain (Crook *et al*, 2000, 2001; Dean *et al*, 1996; Oki *et al*, 2005; Scarr *et al*, 2007; Van Den Beukel *et al*, 1997). It was interesting, therefore, to note that although LY2033298 was an allosteric agonist in ERK1/2 phosphorylation experiments, it had lower efficacy in the NG108-15 cell line and, when used alone, it had minimal effects on receptor internalization. This is an important finding because it indicates that although LY2033298 retains its ability to stimulate certain signaling responses (ie ERK1/2 phosphorylation), when LY2033298 occupies the receptor in the absence of ACh, it does not itself cause the receptor to couple strongly to internalization, which is a key event in the process of receptor desensitization. However, even though the agonist activity of LY2033298 was lower in the NG108-15 cell line, it retained its ability to allosterically potentiate the actions of ACh on the ERK1/2 and internalization pathways in these cells, clearly indicating that its allosteric modulator activity at M<sub>4</sub> mAChRs is fundamental to its actions irrespective of cellular background or receptor expression level. This key finding is underscored by the fact that we also observed a significant effect of LY2033298 on [<sup>3</sup>H]ACh release in rat striatal slices in a largely NMS-sensitive manner, which could only occur if the predominant mode of action of LY2033298 was to potentiate endogenous ACh.

Perhaps most importantly, we have found that the *in vivo* efficacy of LY2033298 to potentiate mAChR agonist-mediated CAR, a model commonly used as a predictor of antipsychotic drug efficacy, was significantly attenuated in M<sub>4</sub> mAChR KO mice. However, we also made the intriguing observation that the actions of LY2033298 in this model were not completely abolished in M<sub>4</sub> mAChR KO mice. As described in our prior study (Chan *et al*, 2008), it is difficult to observe *in vivo* behavioral effects of LY2033298 alone in rodents because of a lower potency of the modulator in potentiating ACh at the rodent M<sub>4</sub> mAChR compared with the human receptor and/or decreased CNS penetrance because of pharmacokinetic limitations. Consequently, this necessitates the administration of a submaximal dose of oxotremorine to provide additional cholinergic tone *in vivo*, thus revealing the allosteric effect. However, the probe-dependent nature of allosteric interactions means that there is a possibility of LY2033298 and oxotremorine interacting at a non-M<sub>4</sub> mAChR subtype, even though this is not possible for the interaction between ACh and LY2033298 (Chan *et al*, 2008). Further studies are currently underway in our laboratory to address this issue. Nonetheless, the significant blunting of *in vivo* activity of LY2033298 in the M<sub>4</sub> mAChR KO mice validates the M<sub>4</sub> mAChR as an important, if not the sole, target for the *in vivo* actions of LY2033298.

In conclusion, we have shown that the novel small molecule allosteric modulator, LY2033298, exerts both agonistic and modulator effects through a common site on the M<sub>4</sub> mAChR that overlaps with the region used by prototypical modulators such as C<sub>7</sub>/3-phth. The modulator is also able to differentially traffic stimuli imparted to the receptor by the endogenous agonist, ACh, highlighting a novel use of allosteric ligands to engender pathway selectivity in addition to orthosteric ligand and receptor subtype selectivity. Importantly, behavioral studies in M<sub>4</sub> mAChR KO mice further validate this receptor as a novel target for the potential treatment of disorders such as psychosis.



## ACKNOWLEDGEMENTS

This work was funded by Program Grant 519461 of the National Health and Medical Research Council (NHMRC) of Australia. AC is a Senior and PMS, a Principal, Research Fellow of the NHMRC. We thank Dr Vimesh Avlani for performing the HEK293 TRex experiments, Dr Celine Valant for the synthesis of C<sub>7</sub>/3-phth, Professor Bryan L Roth for the provision of the M<sub>4</sub> Y<sup>113</sup>C/A<sup>203</sup>G mAChR cDNA, Mr David George for performing the GSK-3 $\beta$  experiments, and Dr Michael Crouch and TGR Biosciences for the generous gifts of ERK1/2 and GSK-3 $\beta$  assay kits.

## DISCLOSURE

Drs Felder, McKinzie, Mogg, and Shaw are employees of Eli Lilly and Co. Professors Christopoulos and Sexton are consultants and Scientific Advisory Board (SAB) members for Addex Pharmaceuticals and have had contracts with GlaxoSmithKline, Pfizer, and Addex for the study of GPCR allosteric modulators. In the past 5 years, Professor Christopoulos has also been a consultant for Amgen, BristolMyersSquibb, and Alchemia and is a member of the Alchemia SAB.

## REFERENCES

- Armbruster BN, Li X, Pausch MH, Herlitze S, Roth BL (2007). Evolving the lock to fit the key to create a family of G protein-coupled receptors potentially activated by an inert ligand. *Proc Natl Acad Sci USA* **104**: 5163–5168.
- Beaulieu JM, Gainetdinov RR, Caron MG (2009). Akt/GSK3 signaling in the action of psychotropic drugs. *Annu Rev Pharmacol Toxicol* **49**: 327–347.
- Beaulieu JM, Sotnikova TD, Yao WD, Kockeritz L, Woodgett JR, Gainetdinov RR et al. (2004). Lithium antagonizes dopamine-dependent behaviors mediated by an AKT/glycogen synthase kinase 3 signaling cascade. *Proc Natl Acad Sci USA* **101**: 5099–5104.
- Bernard V, Normand E, Bloch B (1992). Phenotypical characterization of the rat striatal neurons expressing muscarinic receptor genes. *J Neurosci* **12**: 3591–3600.
- Birdsall NJ, Burgen AS, Hulme EC, Stockton JM, Zigmond MJ (1983). The effect of McN-A-343 on muscarinic receptors in the cerebral cortex and heart. *Br J Pharmacol* **78**: 257–259.
- Black J (1996). A personal view of pharmacology. *Annu Rev Pharmacol Toxicol* **36**: 1–33.
- Bodick NC, Offen WW, Levey AI, Cutler NR, Gauthier SG, Satlin A et al. (1997a). Effects of xanomeline, a selective muscarinic receptor agonist, on cognitive function and behavioral symptoms in Alzheimer disease. *Arch Neurol* **54**: 465–473.
- Bodick NC, Offen WW, Shannon HE, Satterwhite J, Lucas R, van Lier R et al. (1997b). The selective muscarinic agonist xanomeline improves both the cognitive deficits and behavioral symptoms of Alzheimer disease. *Alzheimer Dis Assoc Disord* **11**(Suppl 4): S16–S22.
- Bymaster FP, McKinzie DL, Felder CC, Wess J (2003). Use of M1–M5 muscarinic receptor knockout mice as novel tools to delineate the physiological roles of the muscarinic cholinergic system. *Neurochem Res* **28**: 437–442.
- Chan WY, D LM, Bose S, S NM, J MW, Thompson RC et al. (2008). Allosteric modulation of the muscarinic M4 receptor as an approach to treating schizophrenia. *Proc Natl Acad Sci USA* **105**: 10978–10983.
- Christopoulos A (1998). Assessing the distribution of parameters in models of ligand-receptor interaction: to log or not to log. *Trends Pharmacol Sci* **19**: 351–357.
- Christopoulos A, El-Fakahany EE (1999). Qualitative and quantitative assessment of relative agonist efficacy. *Biochem Pharmacol* **58**: 735–748.
- Christopoulos A, Sorman JL, Mitchelson F, El-Fakahany EE (1999). Characterization of the subtype selectivity of the allosteric modulator heptane-1,7-bis-(dimethyl-3'-phthalimidopropyl) ammonium bromide (C7/3-phth) at cloned muscarinic acetylcholine receptors. *Biochem Pharmacol* **57**: 171–179.
- Conn PJ, Christopoulos A, Lindsley CW (2009). Allosteric modulators of GPCRs: a novel approach for the treatment of CNS disorders. *Nat Rev Drug Discov* **8**: 41–54.
- Crook JM, Tomaskovic-Crook E, Copolov DL, Dean B (2000). Decreased muscarinic receptor binding in subjects with schizophrenia: a study of the human hippocampal formation. *Biol Psychiatry* **48**: 381–388.
- Crook JM, Tomaskovic-Crook E, Copolov DL, Dean B (2001). Low muscarinic receptor binding in prefrontal cortex from subjects with schizophrenia: a study of Brodmann's areas 8, 9, 10, and 46 and the effects of neuroleptic drug treatment. *Am J Psychiatry* **158**: 918–925.
- Dean B, Crook JM, Opeskin K, Hill C, Keks N, Copolov DL (1996). The density of muscarinic M1 receptors is decreased in the caudate-putamen of subjects with schizophrenia. *Mol Psychiatry* **1**: 54–58.
- Deng C, Huang XF (2005). Decreased density of muscarinic receptors in the superior temporal gyrus in schizophrenia. *J Neurosci Res* **81**: 883–890.
- Dwivedi Y, Rizavi HS, Roberts RC, Conley RC, Tamminga CA, Pandey GN (2001). Reduced activation and expression of ERK1/2 MAP kinase in the post-mortem brain of depressed suicide subjects. *J Neurochem* **77**: 916–928.
- Ellis J, Seidenberg M, Brann MR (1993). Use of chimeric muscarinic receptors to investigate epitopes involved in allosteric interactions. *Mol Pharmacol* **44**: 583–588.
- Emamian ES, Hall D, Birnbaum MJ, Karayiorgou M, Gogos JA (2004). Convergent evidence for impaired AKT1–GSK3 $\beta$  signaling in schizophrenia. *Nat Genet* **36**: 131–137.
- Feng P, Guan Z, Yang X, Fang J (2003). Impairments of ERK signal transduction in the brain in a rat model of depression induced by neonatal exposure of clomipramine. *Brain Res* **991**: 195–205.
- Gnagay AL, Seidenberg M, Ellis J (1999). Site-directed mutagenesis reveals two epitopes involved in the subtype selectivity of the allosteric interactions of gallamine at muscarinic acetylcholine receptors. *Mol Pharmacol* **56**: 1245–1253.
- Gomez J, Zhang L, Kostenis E, Felder C, Bymaster F, Brodtkin J et al. (1999). Enhancement of D1 dopamine receptor-mediated locomotor stimulation in M(4) muscarinic acetylcholine receptor knockout mice. *Proc Natl Acad Sci USA* **96**: 10483–10488.
- Gregory KJ, Sexton PM, Christopoulos A (2007). Allosteric modulation of muscarinic acetylcholine receptors. *Curr Neuropharmacol* **5**: 157–167.
- Hall DA (2000). Modeling the functional effects of allosteric modulators at pharmacological receptors: an extension of the two-state model of receptor activation. *Mol Pharmacol* **58**: 1412–1423.
- Hasselmo ME (2006). The role of acetylcholine in learning and memory. *Curr Opin Neurobiol* **16**: 710–715.
- Hasselmo ME, Giocomo LM (2006). Cholinergic modulation of cortical function. *J Mol Neurosci* **30**: 133–135.
- Huang XP, Prilla S, Mohr K, Ellis J (2005). Critical amino acid residues of the common allosteric site on the M2 muscarinic acetylcholine receptor: more similarities than differences between the structurally divergent agents gallamine and bis(ammonio)

- alkane-type hexamethylene-bis-[dimethyl-(3-phthalimidopropyl) ammonium]dibromide. *Mol Pharmacol* **68**: 769–778.
- Ikedo M, Iwata N, Suzuki T, Kitajima T, Yamanouchi Y, Kinoshita Y *et al.* (2004). Association of AKT1 with schizophrenia confirmed in a Japanese population. *Biol Psychiatry* **56**: 698–700.
- Ince E, Ciliax BJ, Levey AI (1997). Differential expression of D1 and D2 dopamine and m4 muscarinic acetylcholine receptor proteins in identified striatonigral neurons. *Synapse* **27**: 357–366.
- Jones CK, Brady AE, Davis AA, Xiang Z, Bubser M, Tantawy MN *et al.* (2008). Novel selective allosteric activator of the M1 muscarinic acetylcholine receptor regulates amyloid processing and produces antipsychotic-like activity in rats. *J Neurosci* **28**: 10422–10433.
- Kenakin T (2007). Collateral efficacy in drug discovery: taking advantage of the good (allosteric) nature of 7TM receptors. *Trends Pharmacol Sci* **28**: 407–415.
- Krejci A, Tucek S (2001). Changes of cooperativity between N-methylscopolamine and allosteric modulators alcuronium and gallamine induced by mutations of external loops of muscarinic M(3) receptors. *Mol Pharmacol* **60**: 761–767.
- Langmead CJ, Christopoulos A (2006). Allosteric agonists of 7TM receptors: expanding the pharmacological toolbox. *Trends Pharmacol Sci* **27**: 475–481.
- Langmead CJ, Fry VA, Forbes IT, Branch CL, Christopoulos A, Wood MD *et al.* (2006). Probing the molecular mechanism of interaction between 4-n-butyl-1-[4-(2-methylphenyl)-4-oxo-1-butyl]-piperidine (AC-42) and the muscarinic M(1) receptor: direct pharmacological evidence that AC-42 is an allosteric agonist. *Mol Pharmacol* **69**: 236–246.
- Lanzafame AA, Sexton PM, Christopoulos A (2006). Interaction studies of multiple binding sites on m4 muscarinic acetylcholine receptors. *Mol Pharmacol* **70**: 736–746.
- Lazareno S, Popham A, Birdsall NJ (2000). Allosteric interactions of staurosporine and other indolocarbazoles with N-[methyl-(3)H]scopolamine and acetylcholine at muscarinic receptor subtypes: identification of a second allosteric site. *Mol Pharmacol* **58**: 194–207.
- Lazareno S, Popham A, Birdsall NJ (2002). Analogs of WIN 62,577 define a second allosteric site on muscarinic receptors. *Mol Pharmacol* **62**: 1492–1505.
- Leach K, Sexton PM, Christopoulos A (2007). Allosteric GPCR modulators: taking advantage of permissive receptor pharmacology. *Trends Pharmacol Sci* **28**: 382–389.
- Leppik RA, Miller RC, Eck M, Paquet JL (1994). Role of acidic amino acids in the allosteric modulation by gallamine of antagonist binding at the m2 muscarinic acetylcholine receptor. *Mol Pharmacol* **45**: 983–990.
- Lovestone S, Killick R, Di Forti M, Murray R (2007). Schizophrenia as a GSK-3 dysregulation disorder. *Trends Neurosci* **30**: 142–149.
- May LT, Avlani VA, Langmead CJ, Herdon HJ, Wood MD, Sexton PM *et al.* (2007a). Structure-function studies of allosteric agonism at M2 muscarinic acetylcholine receptors. *Mol Pharmacol* **72**: 463–476.
- May LT, Leach K, Sexton PM, Christopoulos A (2007b). Allosteric modulation of G protein-coupled receptors. *Annu Rev Pharmacol Toxicol* **47**: 1–51.
- May LT, Lin Y, Sexton PM, Christopoulos A (2005a). Regulation of M2 muscarinic acetylcholine receptor expression and signaling by prolonged exposure to allosteric modulators. *J Pharmacol Exp Ther* **312**: 382–390.
- May LT, Sexton PM, Christopoulos A (2005b). Effects of urea pretreatment on the binding properties of adenosine A1 receptors. *Br J Pharmacol* **146**: 1119–1129.
- Motulsky H, Christopoulos A (2004). *Fitting Models to Biological Data Using Linear and Nonlinear Regression. A Practical Guide to Curve Fitting*. Oxford University Press: New York.
- Nassif-Makki T, Trankle C, Zlotos D, Bejeuhr G, Cambareri A, Pfletschinger C *et al.* (1999). Bisquaternary ligands of the common allosteric site of M2 acetylcholine receptors: search for the minimum essential distances between the pharmacophoric elements. *J Med Chem* **42**: 849–858.
- Nawaratne V, Leach K, Suratman N, Loiacono RE, Felder CC, Armbruster BN *et al.* (2008). New insights into the function of M4 muscarinic acetylcholine receptors gained using a novel allosteric modulator and a ‘designer receptor exclusively activated by a designer drug’(DREADD). *Mol Pharmacol* **74**: 1119–1131.
- Oki T, Takagi Y, Inagaki S, Taketo MM, Manabe T, Matsui M *et al.* (2005). Quantitative analysis of binding parameters of [3H]N-methylscopolamine in central nervous system of muscarinic acetylcholine receptor knockout mice. *Brain Res Mol Brain Res* **133**: 6–11.
- Prilla S, Schrobang J, Ellis J, Holtje HD, Mohr K (2006). Allosteric interactions with muscarinic acetylcholine receptors: complex role of the conserved tryptophan M2422Trp in a critical cluster of amino acids for baseline affinity, subtype selectivity, and cooperativity. *Mol Pharmacol* **70**: 181–193.
- Rorick-Kehn LM, Johnson BG, Knitowski KM, Salhoff CR, Witkin JM, Perry KW *et al.* (2007). *In vivo* pharmacological characterization of the structurally novel, potent, selective mGlu2/3 receptor agonist LY404039 in animal models of psychiatric disorders. *Psychopharmacology (Berl)* **193**: 121–136.
- Scarr E, Sundram S, Keriakous D, Dean B (2007). Altered hippocampal muscarinic M4, but not M1, receptor expression from subjects with schizophrenia. *Biol Psychiatry* **61**: 1161–1170.
- Shekhar A, Potter WZ, Lightfoot J, Lienemann J, Dube S, Mallinckrodt C *et al.* (2008). Selective muscarinic receptor agonist xanomeline as a novel treatment approach for schizophrenia. *Am J Psychiatry* **165**: 1033–1039.
- Shirey JK, Xiang Z, Orton D, Brady AE, Johnson KA, Williams R *et al.* (2008). An allosteric potentiator of M4 mAChR modulates hippocampal synaptic transmission. *Nat Chem Biol* **4**: 42–50.
- Spalding TA, Ma JN, Ott TR, Friberg M, Bajpai A, Bradley SR *et al.* (2006). Structural requirements of transmembrane domain 3 for activation by the M1 muscarinic receptor agonists AC-42, AC-260584, clozapine, and N-desmethyloclozapine: evidence for three distinct modes of receptor activation. *Mol Pharmacol* **70**: 1974–1983.
- Sur C, Mallorga PJ, Wittmann M, Jacobson MA, Pascarella D, Williams JB *et al.* (2003). N-desmethyloclozapine, an allosteric agonist at muscarinic 1 receptor, potentiates N-methyl-D-aspartate receptor activity. *Proc Natl Acad Sci USA* **100**: 13674–13679.
- Tzavara ET, Bymaster FP, Davis RJ, Wade MR, Perry KW, Wess J *et al.* (2004). M4 muscarinic receptors regulate the dynamics of cholinergic and dopaminergic neurotransmission: relevance to the pathophysiology and treatment of related CNS pathologies. *FASEB J* **18**: 1410–1412.
- Urban JD, Clarke WP, von Zastrow M, Nichols DE, Kobilka B, Weinstein H *et al.* (2007). Functional selectivity and classical concepts of quantitative pharmacology. *J Pharmacol Exp Ther* **320**: 1–13.
- Valant C, Gregory KJ, Hall NE, Scammells PJ, Lew MJ, Sexton PM *et al.* (2008). A novel mechanism of G protein-coupled receptor functional selectivity Muscarinic partial agonist McN-A-343 as a bitopic orthosteric/allosteric ligand. *J Biol Chem* **283**: 29312–29321.
- Valant C, Sexton PM, Christopoulos A (2009). Orthosteric/allosteric bitopic ligands: going hybrid at GPCRs. *Mol Interv* **9**: 125–135.
- Van Den Beukel I, Dijcks FA, Vanderheyden P, Vauquelin G, Oortgiesen M (1997). Differential muscarinic receptor binding of acetylcholinesterase inhibitors in rat brain, human brain and Chinese hamster ovary cells expressing human receptors. *J Pharmacol Exp Ther* **281**: 1113–1119.

- Voigtlander U, Johren K, Mohr M, Raasch A, Trankle C, Buller S *et al.* (2003). Allosteric site on muscarinic acetylcholine receptors: identification of two amino acids in the muscarinic M2 receptor that account entirely for the M2/M5 subtype selectivities of some structurally diverse allosteric ligands in N-methylscopolamine-occupied receptors. *Mol Pharmacol* **64**: 21–31.
- Wess J, Duttaroy A, Zhang W, Gomeza J, Cui Y, Miyakawa T *et al.* (2003). M1-M5 muscarinic receptor knockout mice as novel tools to study the physiological roles of the muscarinic cholinergic system. *Receptors Channels* **9**: 279–290.
- Wess J, Eglen RM, Gautam D (2007). Muscarinic acetylcholine receptors: mutant mice provide new insights for drug development. *Nat Rev Drug Discov* **6**: 721–733.
- Zhang W, Basile AS, Gomeza J, Volpicelli LA, Levey AI, Wess J (2002a). Characterization of central inhibitory muscarinic autoreceptors by the use of muscarinic acetylcholine receptor knock-out mice. *J Neurosci* **22**: 1709–1717.
- Zhang W, Yamada M, Gomeza J, Basile AS, Wess J (2002b). Multiple muscarinic acetylcholine receptor subtypes modulate striatal dopamine release, as studied with M1-M5 muscarinic receptor knock-out mice. *J Neurosci* **22**: 6347–6352.

Supplementary Information accompanies the paper on the Neuropsychopharmacology website (<http://www.nature.com/npp>)